Mechatronics 31 (2015) 22–29

Contents lists available at ScienceDirect

Mechatronics

journal homepage: www.elsevier.com/locate/mechatronics

A new method based on Fiber Bragg grating sensor for the milling force measurement

Mingyao Liu, Zhijian Zhang *, Zude Zhou, Shuang Peng, Yuegang Tan

School of Mechanical and Electronic Engineering, Wuhan University of Technology, Wuhan 430070, China
Hubei Digital Manufacturing Key Laboratory, Wuhan 430070, China

ARTICLE INFO

Article history:
Received 30 October 2014
Revised 11 March 2015
Accepted 17 March 2015
Available online 1 April 2015

Keywords:
Milling force
Fiber Bragg grating sensor
Annulus elastic body

ABSTRACT

Milling force is an important parameter to describe the mechanical processing chip removal process, and it has a direct influence on generation of heat, tool wear or failure, quality of machined surface and accuracy of the work piece. Its accurate measurement is a significant basis for judging process state and improving the reliability of machining system. In this study, through analyzing the variation rule of ring diameter, a new method that using Fiber Bragg grating sensors and variation rule of ring diameter to measure the milling force has been proposed, and the basic structure of annulus has also been designed. A dynamometer has also been constructed, and the preliminary verification test was done. Through the analysis of experimental data, the dynamometer based on annulus elastic body can be used in milling force test, and it owns high sensitivity.

1. Introduction

Metal cutting is one of the most momentous manufacturing processes and is used widely in various industries such as automotive, watercraft and project machine. During metal cutting, in order to prolong machine tool service life and prevent tool breakage, mechanical properties of the milling tool should be known and therefore care should be taken to prevent this [1]. Knowledge of cutting forces is important in metal cutting, which should not deform the machine tools, milling tools and tool holders. Milling force measurement is very important in metal cutting field as they are used to determine the processing state of machine tool, achieve the process intelligently and machining process controllable, improve the reliability of machining system. Beside this, the milling force has direct impact on the generation of cutting heat, tool wear, quality of machined surface and accuracy of the work piece [2,3].

The current study on the cutting force is divided into two directions, one of which is the prediction of cutting forces, and the other is the measurement of cutting force. Prediction of the cutting force has significant meaning in choosing appropriate machining parameters and suitable processing conditions; it also can be used in process planning [4,5]. Due to the complex tool configuration/cutting condition of metal cutting operations and some unknown factors and stresses, theoretical cutting force calculations failed to produce accurate results [6]. Therefore, measurement of cutting forces is necessary. In order to obtain accurate cutting force during the machine processing, many scholars have conducted long-term research [7], and studies on cutting force measurement mainly focus on direct measurement of cutting force and indirect measurement of cutting force. Indirect measurement of cutting force is mainly by the way of measuring the spindle motor power or motor current to reflect the change of cutting force [8,9], or measuring the driving motor power or motor current to reflect the change of cutting force [10,11]. The indirect measurement has the advantages of simple structure, convenient installation and required technologies mature, but the interference factors, like mechanical structure, transmission, temperature and others, easily affect the stability of power or current signal, so it is hard to reflect the cutting force precisely. Direct measurement of cutting force usually uses elastic body to convert the cutting force into the strain of elastic body, then utilizing the sensing element to detect the strain. The sensing element commonly used is concentrated in resistance strain gage [1,6,12,13] and piezoelectric element [14–16]. Resistance strain gage possesses high sensitivity, small volume, easy installation, low cost and other merits, however, it also has the characteristics of complex line, wiring difficulty and easily being affected by environment, etc. Besides, the elastic body adopted in the dynamometer based on resistance strain gage is octagonal ring or similar structure of octagonal ring whose measurement accuracy is lower than needed. The main advantage of piezoelectric element is of good rigidity, small volume and quick

* Corresponding author at: School of Mechanical and Electronic Engineering, Wuhan University of Technology, Wuhan 430070, China.
E-mail address: 1183030053@qq.com (Z. Zhang).

http://dx.doi.org/10.1016/j.mechatronics.2015.03.007
0957-4158/

response, but it is very sensitive to temperature changes, humidity and electromagnetic disturbance, and the piezoelectric element itself has hysteresis characteristics, which cannot meet the cutting force test environment. In order to adapt to the complex environment requirements and measure the cutting force accurately, other methods on the cutting force measurement are also explored. Ref. [17] uses Fiber Bragg Grating (FBG) sensors to measure cutting force; however the FBG sensors were directly pasted on the tool bar of turning tool which is easily influenced by temperature.

Compared with traditional sensors, FBG sensors are light in weight, small in volume, high in precision, immune to electromagnetic, resistant to corrosion and easy to conduct distributer dynamic measurement. The research group studied the theory of strain measurement of FBG sensor, and developed a dynamometer based on FBG sensor and octagonal ring [18]. Owing to the limitation of measurement sensitivity of octagonal ring, a dynamometer based on FBG sensor failed to meet the requirements. At the same time, influenced by pasting skill, there is adhesive layer between sensor and the surface of octagonal ring, and the thickness of adhesive layer is uneven [19]. What's more, the elastic modulus of adhesive layer and the bare optical fiber generally varies greatly, and this resulting in the strain measured by sensor and the real strain of the surface of the octagonal ring are different. It has a great effect on the measurement precision of the dynamometer. Because of the poor reproducibility of pasting skills, multiple measurement points' strain transfer ratios, which are the ratio of measured strain of FBG sensor to the real strain of measured point, are different from each other, so it is difficult to distinguish the reliability of measured data. Because the sensor itself has a certain size, like length and width, and the contact between the sensor and the octagonal ring is an area, rather than a point, all of which lead to the strain of sensor perception is the average strain of the contact surface not equal to the strain nodes. Beside the strain nodes, all other points of strain are caused by multiple direction forces, so it is quite difficult to work out the external applied loads when the measured strain is not the strain of strain nodes.

In this paper, by analyzing the variation rule of ring diameter, a new method that using FBG and variation rule of ring diameter to measure the milling force has been proposed, and the basic structure of annulus elastic body and pre-tightening device has also been designed. Owing to the grating part of FBG sensor does not need to be pasted on the surface of elastic body, so annulus elastic body is capable of measuring strain without being limited by the pasted skill and pasted area. Besides, the strength of annulus elastic body has been checked, and the static frequency of annulus elastic body which is a clear limitation threshold for the useful has also been studied. For the sake of obtaining the basic properties of annulus elastic body, several tests have also been done.

2. The principle of measuring milling force

2.1. Measurement theory of FBG

Fiber Bragg grating sensor uses photosensitive properties of fiber materials, thus only certain wavelengths of light will be reflected back when broadband spectra via grating, the rest of the light will pass through the grating, as is shown in Fig. 1. The reflected light wavelength of grating λ_B mainly relies on the fiber grating period Λ and effective refractive index n_{eff}, it can be calculated by the following equations:

$$\lambda_B = 2n_{eff}\Lambda \tag{1}$$

Under the influence of stress strain or temperature, effective refractive index of fiber grating and the fiber grating period will change. The wavelength of light that being reflected by grating will change from λ_{B_0} to λ_B, so it can be considered as a function of strain σ and temperature T, and its change can be calculated as follows:

$$\Delta\lambda_B = \lambda_B(\sigma, T) - \lambda_{B_0}(\sigma_0, T_0) \tag{2}$$

Make the formula (1) as a Taylor expansion and take the first order approximation, and pull in Young's modulus of Fiber Y_F, thermal expansion coefficient α_Λ, thermo-optic coefficient α_n and photo elasticity coefficient P_e, then the wavelength shift can be expressed in the following equation:

$$\Delta\lambda_B = \lambda_B[(1 - P_e)\Delta\varepsilon + (\alpha_\Lambda + \alpha_n)\Delta T] \tag{3}$$

where $\Delta\varepsilon$ represents the variation of axial strain of Optical fiber; ΔT represents the change of temperature, which is equal to $\Delta\sigma/Y_F$; $\Delta\sigma$ represents the change of axial stress of Optical fiber.

The wavelength of fiber and temperature changes can be measured by test, then utilizing the formula (3) can get the strain of corresponding measured point.

2.2. The principle of measuring milling force

When the radius of the ring far outweighs the thickness of it, for the sake of simplifying the calculation, it can be simplified into a thin ring. Deformation of ring under external loads is shown in Fig. 2.

Under the action of vertical force F_t, points C and D are the largest strain points, however, the strain of E, F, G and H points is zero. Under the action of horizontal force F_c, the strain of C and D points is zero, however, the strain of E, F, G and H points is the largest strain points. Under the action of external force, these special points on ring are called strain nodes. According to the knowledge of Mechanics material, the relative displacement between two points located on the same diameter of one ring can be figured out. A method that using FBG and variation rule of ring diameter to measure the milling force has been proposed. The diameter of bare Fiber is only 0.125 mm, so both ends of FBG can be fixed in the two strain nodes located at one diameter of ring. The FBG is respectively arranged between C and D points, E and F points and G and H points, the magnitude and direction of external loads can be obtained through measuring the strain of FBG when it is stretched or compressed.

3. The variation rule of ring diameter

3.1. The deformation analysis of ring under the action of vertical force

The deformation of ring under the action of vertical force F_t is shown in the Fig. 3.

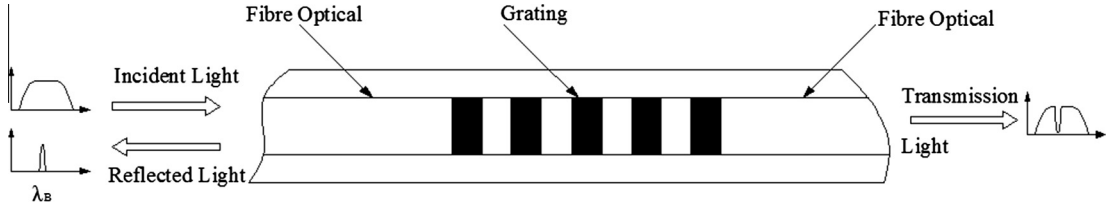

Fig. 1. Fiber Bragg Grating sensor.

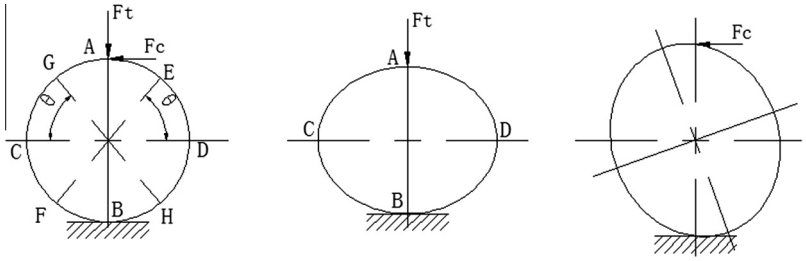

Fig. 2. Deformation of ring under external loads.

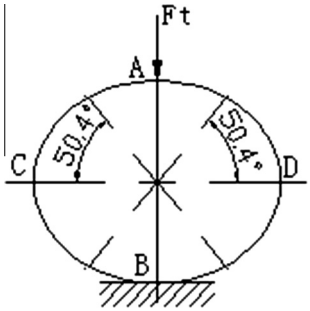

Fig. 3. Ring under vertical direction force.

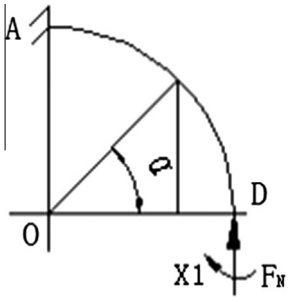

Fig. 4. 1/4 Ring.

In order to calculate the relative displacement between two points, the bending moment of any point on ring need to be worked out. Owing to ring under the action of vertical force is still symmetric structure, so we can just choose 1/4 ring to analyze as shown in the Fig. 4.

AD parts are still basic static system, the rotation angle of D point along the $X1$ direction is zero. Choosing δ_{11} as the rotation angle of D point along the $X1$ direction under the action of $X1 = 1$, similarly, choosing Δ_{1F} as the rotation angle of D point along the $X1$ direction under the action of $F_N = F_t/2$, then canonical equation can be expressed as follows:

$$\delta_{11}X_1 + \Delta_{1F} = 0 \tag{4}$$

The bending moment of any point under the action of F_N on the ring can be expressed as follows:

$$M_{F_N}(\alpha) = \frac{-F_tR(1 - Cos\alpha)}{2} \quad 0 \leqslant \alpha \leqslant \pi/2 \tag{5}$$

Taking Elastic Modulus E, Moment of inertia I and Radius (R) of ring into account, Δ_{1F} and δ_{11} are expressed as:

$$\delta_{11} = \frac{\pi R}{2EI} \tag{6}$$

$$\Delta_{1F} = -\frac{F_tR^2}{2EI}\left(\frac{\pi}{2} - 1\right) \tag{7}$$

where Moment of inertia I is equal to $bh^3/12$; b is the width of ring cross section; h is the thickness of ring cross section.

Then the bending moment of any point on 1/4 ring can be obtained from the following formula:

$$M_t(\alpha) = F_tR\left(\frac{Cos\alpha}{2} - \frac{1}{\pi}\right) \quad 0 \leqslant \alpha \leqslant \pi/2 \tag{8}$$

In order to calculate the relative displacement between two points C and D, unit forces in the opposite direction which along the diameter were respectively applied at points C and D, as shown in Fig. 5.

By using Mohr integration, just like the above, the bending moment of any point on 1/4 ring under the action of unit forces can be calculated by using the following formula:

$$\overline{M_t(\alpha)_{CD}} = R\left(\frac{1}{\pi} - \frac{Sin\alpha}{2}\right) \quad 0 \leqslant \alpha \leqslant \pi/2 \tag{9}$$

The bending moment of any point on the other 3/4 ring can be figured out by the way of the above. By using the Mohr integration, the relative displacement between points C and D can be obtained from the following relation:

$$\delta_{CD_t} = 0.1369\frac{F_tR^3}{EI} \tag{10}$$

In order to calculate the relative displacement between points E and F, unit forces in the opposite direction which along the diameter were respectively applied at points E and F. The bending moment of any point on ring under the action of unit forces can be figured out. The relative displacement between points E and F can be calculated as follows:

$$\delta_{EF_t} = 0.0334\frac{F_tR^3}{EI} \tag{11}$$

Under the action of vertical direction force, the ring is still a symmetric structure, so the relative displacement between points G and H is equal to the relative displacement between points C and D:

$$\delta_{GH_t} = 0.0334\frac{F_tR^3}{EI} \tag{12}$$

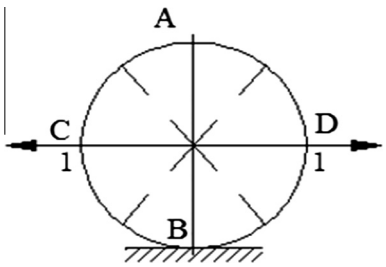

Fig. 5. Apply unit force at points C and D.

3.2. The deformation analysis of ring under the action of horizontal force

The deformation of ring under the action of horizontal force F_c is shown in the Fig. 6.

In order to calculate the relative displacement between two points, the bending moment of any point on ring need to be worked out. Owing to ring under the action of horizontal force is asymmetric structure, so we can but choose the whole ring to analyze. Because the B point is fastened to the bottom, so the displacement of B point along the horizontal and the vertical direction is zero and the rotation angle of cross section of B point is zero. For obtaining the bending moment, the left side of the cross section of B point still be saw as fixed end, but the right side of the cross of B point is saw as movable end, as shown in Fig. 7.

The bending moment of any point on ring under the action of horizontal force can be calculated by the following equation:

$$M_{F_c}(\beta) = -F_c R(1 + Cos\beta) \quad \pi \leqslant \beta \leqslant 2\pi \tag{13}$$

Similarly, under the action of $Y1$, $Y2$, and $Y3$ respectively, the bending moment of any point on ring can be expressed as:

$$\overline{M_{c1}(\beta)} = -1 \quad 0 \leqslant \beta \leqslant 2\pi \tag{14}$$

$$\overline{M_{c2}(\beta)} = -R(1 - Cos\beta) \quad 0 \leqslant \beta \leqslant 2\pi \tag{15}$$

$$\overline{M_{c3}(\beta)} = RSin\beta \quad 0 \leqslant \beta \leqslant 2\pi \tag{16}$$

Like the above formula (6) and (7), $\delta_{ij}(i,j = 1,2,3)$ and $\Delta_{iF}(i = 1,2,3)$ can be figured out by using Mohr integration, then we can get the canonical equation as follows:

$$\begin{cases} \delta_{11}Y_1 + \delta_{12}Y_2 + \delta_{13}Y_3 + \Delta_{1F} = 0 \\ \delta_{21}Y_1 + \delta_{22}Y_2 + \delta_{23}Y_3 + \Delta_{2F} = 0 \\ \delta_{31}Y_1 + \delta_{32}Y_2 + \delta_{23}Y_3 + \Delta_{3F} = 0 \end{cases} \tag{17}$$

By using canonical equation, the bending moment of any point on ring can be obtained from the relation:

$$M_c(\beta) = \begin{cases} F_c R\left(\frac{1+Cos\beta}{2} - \frac{2Sin\beta}{\pi}\right) & 0 \leqslant \beta \leqslant \pi \\ -F_c R\left(\frac{1+Cos\beta}{2} + \frac{2Sin\beta}{\pi}\right) & \pi \leqslant \beta \leqslant 2\pi \end{cases} \tag{18}$$

Unit forces in opposite direction which along the diameter were respectively applied at points C and D, then the bending moment of any point on ring was calculated out. The relative displacement between points C and D can be calculated by using the following equation:

$$\delta_{CD_c} = 0 \tag{19}$$

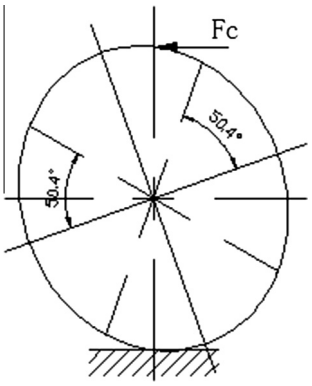

Fig. 6. Ring under horizontal direction force.

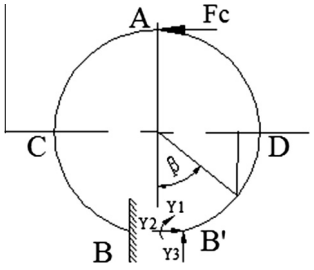

Fig. 7. The analysis of ring under horizontal direction force.

In order to calculate the relative displacement between points E and F, unit forces in opposite direction which along the diameter were respectively applied at points E and F. Then the bending moment of any point on ring under the action of unit forces can be figured out. The relative displacement between points E and F can be calculated by using the following equation:

$$\delta_{EF_c} = -0.2802\frac{F_c R^3}{EI} \tag{20}$$

In order to calculate the relative displacement between points G and H, unit forces in opposite direction which along the diameter were respectively applied at points G and H. Similar to the above, the relative displacement between points G and H can be calculated by using the following equation:

$$\delta_{EF_c} = 1.0796\frac{F_c R^3}{EI} \tag{21}$$

3.3. The deformation analysis of ring under the action of vertical and horizontal forces

Under the action of vertical and horizontal forces, the relative displacements between points C and D, E and F and G and H can be calculated as follows:

$$\begin{cases} \delta_{CD} = 0.1369\frac{F_t R^3}{EI} \\ \delta_{EF} = (0.0334F_t - 0.2802F_c)\frac{R^3}{EI} \\ \delta_{GH} = (0.0334F_t + 1.0796F_c)\frac{R^3}{EI} \end{cases} \tag{22}$$

4. The annulus structure design and parameters determination

4.1. The annulus structure design

In order to measure the relative displacement between two strain nodes, both ends of FBG sensor need to pass through two points of annulus on the same diameter and pasted in the small holes located at the annulus or slider whose diameter is less than one millimeter, instead of pasting the grating part of FBG sensor to the measured structure. The annulus will generate elastic deformation under the action of external forces, then two ends of Grating sensors will be stretched or compressed in which the FBG sensor can get the value of external forces. The cross sectional area of FBG sensor is 4.86625×10^{-8} m^2 which is small enough to be ignored, so this elastic body is, although similar to octagonal ring, capable of measuring strain without being limited by the pasted skill and pasted area. What's more, the FBG must be preloaded to measure the relative displacement between two strain nodes. For applying preload on the FBG and preventing rotation of FBG during pre-stressing, the pre-tightening device is also needed. From the above analysis, we need three FBGs to measure three relative displacements.

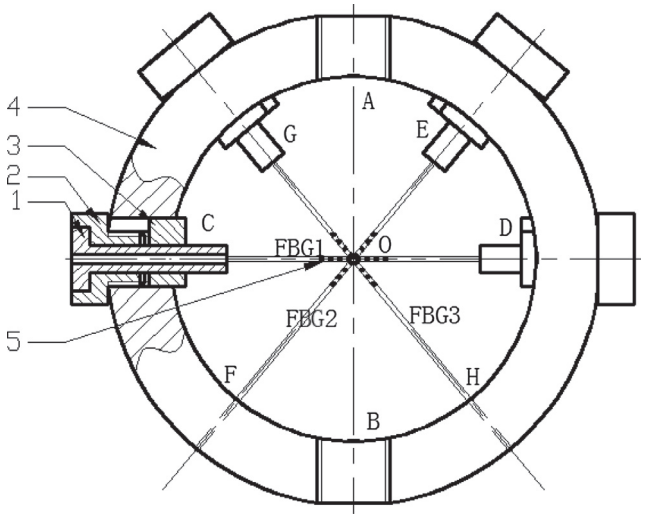

1. Slider 2. Fine adjustment nut 3. Snap ring
4. Annulus elastic body 5. FBG

Fig. 8. Annulus elastic body.

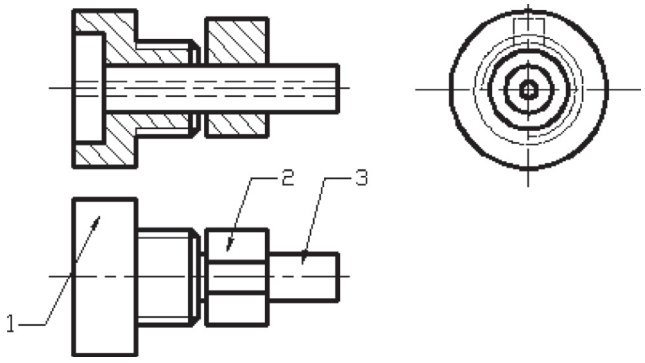

1. Fine adjustment nut 2. Snap ring 3. The slider

Fig. 9. Pre-tightening device.

According to the above requirements, the basic structure of annulus elastic body has been designed as shown in Fig. 8. The pre-tightening device, as shown in Fig. 9, consists of fine adjustment nut, snap ring and slider. The connection between Fine adjustment nut and Slider is transitional connection; the connection between Slider and Snap ring is clearance connection. Fine adjustment nut can be installed to annulus by threaded connection; FBG was passed through the inner hole of slider and fixed in it. We can twist the Fine adjustment nut to drive Slider to move along the axial thread hole. During this period, snap ring can prevent Slider rotation, so FBG will not be twisted.

4.2. The parameters of annulus

The basic performance index of elastic body is static stiffness, sensitivity and natural frequency. Static stiffness shows the ability of resisting deformation of elastic body under the action of external forces, generally the value of static stiffness of a dynamometer should not less than 10^7 N/m. Sensitivity is an important index of dynamometer, and usually using με/N to reflect the sensitivity of dynamometer. Natural frequency of dynamometer is at least four times than the vibration frequency of the machine and should be as high as possible.

The values of static stiffness K, sensitivity S and natural frequency f of annulus elastic body are given as in the following equation:

$$K = \frac{Ebh^3}{1.8R^3} \tag{23}$$

$$f = \frac{1}{2\pi}\sqrt{\frac{K}{m}} \tag{24}$$

$$S = \frac{\delta}{Fl} \tag{25}$$

where K is the ring constant (N/m) of dynamometer; m is the mass (kg) of dynamometer; f is the natural frequency (rev./s) of dynamometer; l is the length of fiber located in the inner of annulus; F is horizontal force F_c or vertical force F_t .

From the above equations, we can come to a conclusion that the value of static stiffness is proportionate to bh^3/R^3 and the value of natural frequency is proportionate to $\sqrt{bh^3/R^3}$, while the value of sensitivity is inversely proportionate to bh^3/R^3. In order to meet the conditions in static stiffness and natural frequency, we should choose the larger R/h and smaller b to obtain higher sensitivity. So the parameters of annulus are R (28 mm), h (7 mm) and b (25 mm).

4.3. The strength check of annulus

As the elastic body is an important part of dynamometer, rigidity and natural frequency should be taken into account when selecting the annulus material. In this study, 45 steel, which meets requirements, was selected as the annulus material. Part of physical and mechanical properties of this material is given in Table 1.

In actual machining process, the maximum milling force is generally not more than 5000 N, so choosing 5000 N as maximum milling force F_m to check the strength of the annulus. Under the action of vertical force and horizontal force respectively, the largest stress can be figured out by using the following equations:

$$\sigma_{t\max} = \frac{1.09F_mR}{bh^2} \tag{26}$$

$$\sigma_{c\max} = \frac{2.31F_mR}{bh^2} \tag{27}$$

The largest stress is $\sigma_{t\max} = 124.5716 \times 10^6$ N/m^2 and $\sigma_{c\max} = 264.0000 \times 10^6$ N/m^2, and they are smaller than allowable tensile stress and allowable compressive stress, then we can know that the annulus owns enough strength.

4.4. The stiffness and natural frequency of annulus

The static stiffness showed the capability of resisting deformation of elastic body under the action of external force, and the static stiffness of annulus elastic body is $K = 4.5572 \times 10^8$. The mass of dynamometer is $m = 11$ kg, then, the value of natural frequency of annulus elastic body can be calculated out by using formula (24), it is $f = 324$ Hz.

Table 1
Properties of 45 steel.

Modulus of elasticity E	2.1×10^{11}
Allowable tensile stress $[\sigma]_c$	600 N/mm^2
Allowable compressive stress $[\sigma]_t$	355 N/mm^2
Density ρ	7.85×10^3 kg/m^3
Poisson's ratio μ	0.3

Vibration frequency of the machine tool to which the dynamometer is mounted for cutting force measurement should conform to the natural frequency of the dynamometer. Vibration frequency of milling machine tool is related to the spindle speed of milling machine tool, and we can get precise values of vibration frequency by measuring [20] or theoretical values by theoretical calculation [1]. Because it does not need high accuracy, the vibration frequency can be obtained easily by the following equation.

$$f_m = \frac{n}{60} \tag{28}$$

where f_m is vibration frequency of milling machine tool; n is the spindle speed of milling machine tool.

In order to prevent resonance and protect the elastic body, the dynamometer should have natural frequency of at least three times the frequency of milling machine tool. Therefore, vibration frequency of the milling machine tool should be less than 108 Hz, so the spindle of the machine tool should not be higher than 6480 rpm.

4.5. Performance comparison between annulus and octagonal rings

4.5.1. The comparison of theoretical sensitivity

By using formula (22) and (25), the value of sensitivity of annulus elastic body is given in the Table 2.

We can get the strain of strain nodes of octagonal ring [13], then the sensitivity can be calculated out, the values of octagonal ring sensitivity are given in the Table 3.

Under the same parameters condition, that is R (28 mm), h (7 mm) and b (25 mm), the comparison of testing sensitivity, calculated out by using the formulas in Tables 3 and 4, between Octagonal ring and Annulus elastic ring is shown in the Table 4.

From Table 4, we can obviously see that the testing sensitivity of annulus elastic body is much higher than the testing sensitivity of octagonal ring.

4.5.2. The comparison of theoretical precision

When we use annulus elastic body to measure milling force, sensors do not need to be stuck to the surface of the annulus elastic body, as is shown in Fig. 10. Without the influence of pasted skill, there is no adhesive layer between strain sensor and the measure point, and there is little difference between the strain measured by sensor and the real strain of the measure point. What's more, without the effect of pasted skill, a plurality of sensors has similar measure precision. Besides, the contact of the sensor and the annulus is a point, rather than an area, the strain of sensor feeling is the strain of the strain nodes, not an average strain of an attached area.

When compared with octagonal, under the case of using the same kind of FBG and Optical Demodulator and Fiber demodulation instrument software, we can easily come to a conclusion that the testing precision of annulus elastic body is way above octagonal ring.

4.5.3. The comparison of the strength of FBG

In dynamometer used of octagonal ring and Fiber Bragg grating, limited by the inaccuracy measurement of packaged FBG, the bare FBG is directly pasted on the surface of the octagonal ring. However, bare FBG is very slender, fragile, and it is difficult to survive in the harsh environment, this makes the dynamometer constructed by octagonal ring is difficult to be used for long-term and on-line monitoring the actual machining process. In dynamometer used of annulus, FBG is not needed to measure strain directly, so it can be encapsulated, and then it is difficult to be damaged.

Table 2
Sensitivity of annulus elastic body.

Under the action of vertical force	Under the action of horizontal force
$S_{CD_t} = 1.6428\frac{R^3}{Ebh^3l}$	$S_{CD_c} = 0$
$S_{EF_t} = 0.4008\frac{R^3}{Ebh^3l}$	$S_{EF_c} = -3.3624\frac{R^3}{Ebh^3l}$
$S_{GH_c} = 0.4008\frac{R^3}{Ebh^3l}$	$S_{GH_c} = 12.9552\frac{R^3}{Ebh^3l}$

Table 3
Sensitivity of octagonal ring.

Under the action of vertical force	Under the action of horizontal force
$S_C = \frac{1.09R}{Ebh^2}$	$S_G = -\frac{2.18R}{Ebh^2}$
$S_D = \frac{1.09R}{Ebh^2}$	$S_E = \frac{2.18R}{Ebh^2}$

Table 4
The comparison of testing sensitivity.

Type of elastic body	Measurement point	Under the action of vertical force	Under the action of horizontal force
Octagonal	S_C	0.1186	0
	S_D	0.1186	0
	S_E	0	0.2373
	S_G	0	−0.2373
Annulus	S_{CD}	0.5136	0
	S_{EF}	0.2572	−1.0511
	S_{GH}	0.2572	4.0494

5. Method and experiment set up

5.1. Dynamometer

A dynamometer capable of measuring three milling forces-main milling force (F_s), feed force (F_f) and radial or thrust force (F_t)-during metal milling was designed and constructed. This dynamometer consists of four elastic rings in which Fiber Bragg grating was fixed, as shown in Fig. 11.

From Fig. 11, we can see that milling force F_x is supported by a and d annulus of the dynamometer; milling force F_y is supported by b and c annulus; milling force F_z that perpendicular to the working plane is supported by a, b, c and d annulus.

5.2. Data acquisition

On-line and real-time information of the milling force data is automatically read and stored by a system during metal milling. Under the action of external force, elastic body gets deformed and converts it into a proportional strain to the external force. Fiber Bragg grating can detect strain and convert it into the change of wavelength of fiber. By Optical Demodulator, changes in optical fiber wavelength can be demodulated into digital signal, and its change can be shown in the Fiber demodulation instrument software and stored into PC. The stored data can be retrieved and used for analysis when required. The list of the experimental equipment used in this study is shown in Table 5.

6. The preliminary verification test

6.1. The preloading of Fiber Bragg grating

Because the value of strain ε_{EF} is, under the action of external load, negative, and we cannot guarantee FBG is in a straight state after it was fixed, so it needs to be preloaded. Connect the optical fiber jumper wire to Optical demodulator, and connect Optical demodulator to computer, then three different FBGs connected to one fiber jumper reflection wavelength can be viewed on the PC. Rotating fine adjustment nut to make optical fiber stretched and produce strain, we must check the change of wavelength

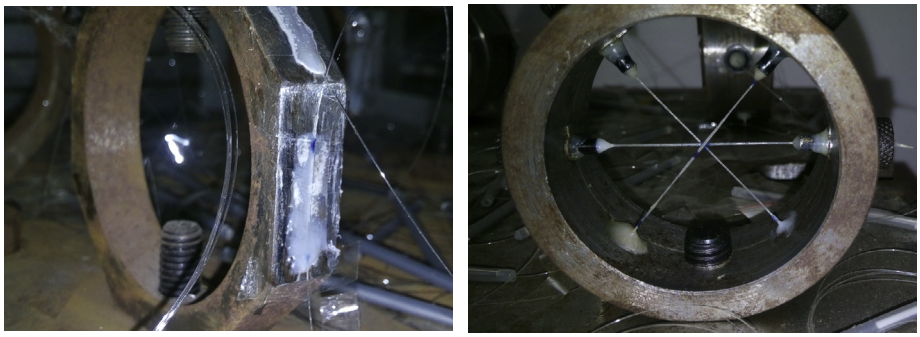

Fig. 10. Octagonal Ring and annulus with FBG sensors.

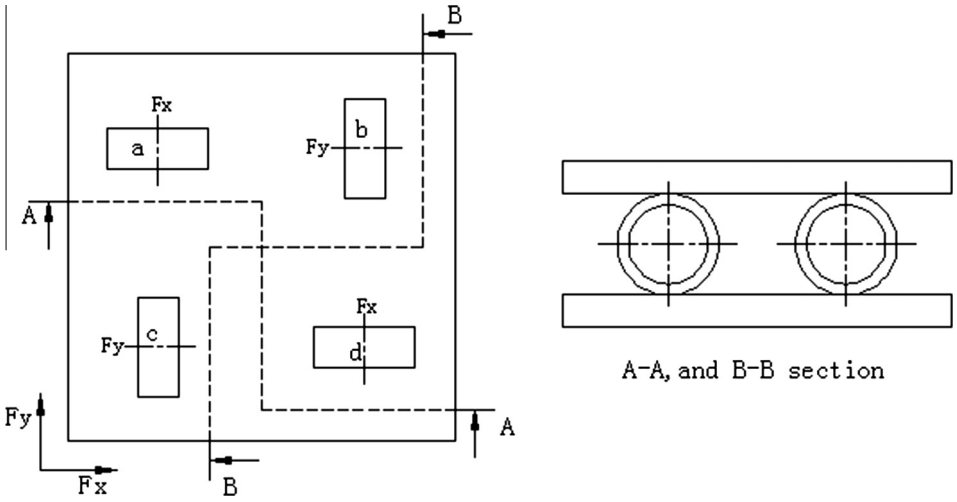

Fig. 11. Dynamometer.

Table 5
Experimental instruments and they performance.

Dynamometer	FBG-based on four-component milling force dynamometer
Ring	Annulus in shape; made of 45#; Width (b = 25 mm), Insider diameter (d = 24.5 mm), Out diameter (D = 31.5 mm)
Fiber Bragg grating	1300 serises of different center wavelength of FBG sensor
Fiber jumper wire	FC type Single-mode Fiber jumper wire; Diameter of fiber core (0.009 mm), Diameter of Optical fiber protective layer (0.125 mm)
Optical Demodulator	Made by WUTOS, Frequency range: 1–3000 Hz, Wavelength resolution: 1 pm
Fiber demodulation instrument software	WHUT High speed optical fiber demodulation system
Loading device	Analog Force Gauge, NK-500, the maximum 500 N, index value 2 N

constantly during this period, and stop rotating when reflection wavelength of FBG reaches a certain value.

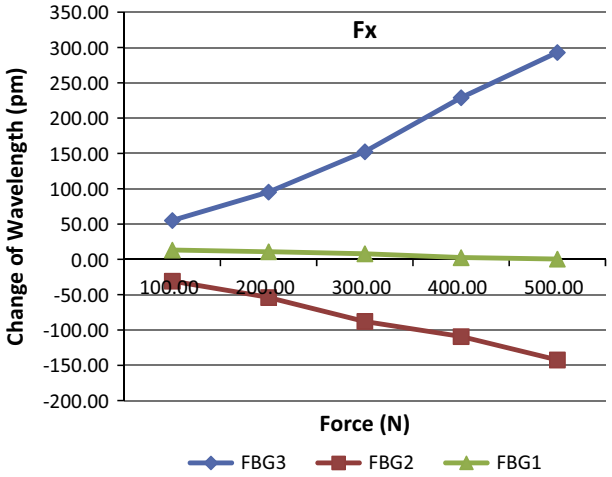

Fig. 12. The change of FBG wavelength of a and d annulus under the action of F_x.

6.2. Preliminary verification test

In order to explore whether or not annulus elastic body can measure milling force, several experiments were done. The experiment was done in three directions for F_x, F_y and F_z. The loads up to 450 N × 90 N intervals were applied for F_z, the loads up to 500 N × 100 N intervals were applied for F_x and F_y, and the values of wavelength of FBG sensors were recorded for each load intervals. In the dynamometer, milling force F_x is supported by a and d annulus; milling force F_y is supported by b and c annulus; milling force F_z that perpendicular to the working plane is supported by a, b, c and d annulus. For the sake of ensuring the accuracy and repeatability of test data, every experiment has been repeated three times. Through the analysis of experimental data, we can get the following data chart.

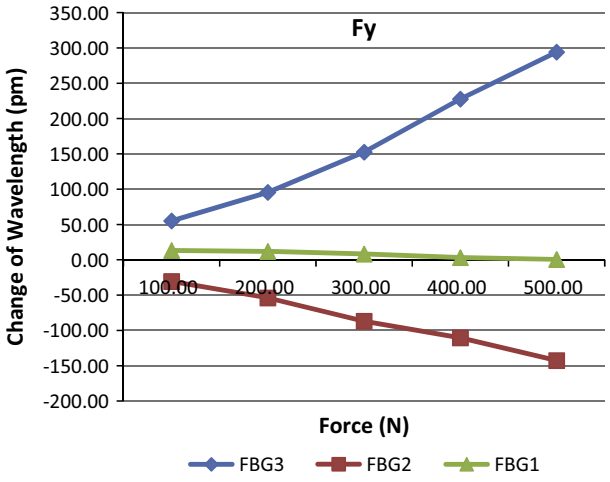

Fig. 13. The change of FBG wavelength of *b* and *c* annulus under the action of F_y.

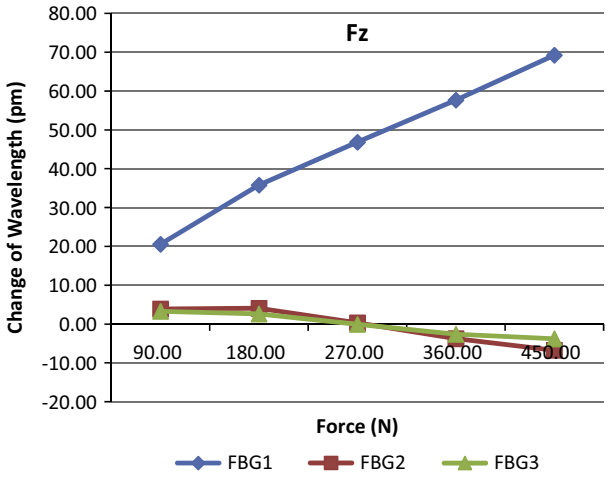

Fig. 14. The change of FBG wavelength of *a*, *b*, *c* and *d* annulus under the action of F_z.

The Figs. 12–14 show that the change of FBG wavelength (1 pm = 1 με) is similar to the variation rule of ring diameter; they certifies that annulus elastic body with high sensitivity can be used in force measurement.

7. Conclusion

In this paper, through analyzing the variation rule of ring diameter, a new method that using FBG and variation rule of ring diameter to measure the milling force has been proposed, and the basic structure of annulus elastic body and pre-tightening device has also been designed. In the annulus body, both ends of FBG sensor are fixed in small holes located at the annulus or slider whose diameter is less than one millimeter, grating part of FBG sensors needs not to be stuck to the surface of the measured matrix, so that it does not exist the problem of grating paste. Besides, the annulus body based on variation rule of ring diameter owns high sensitivity. A dynamometer based on annulus elastic body has also been constructed, and the preliminary verification test has been done. Through the analysis of experimental data, the dynamometer based on annulus elastic body can be used in milling force test, and it owns high sensitivity.

Acknowledgements

This experimental study was supported by the National Natural Science Fund of Chinese (General Program, Grant NO51375359) and Independent Innovation Foundation of Wuhan University of Technology (Grant NO145204010). The authors would like to thank Hubei Digital Manufacturing Key Laboratory (Wuhan University of Technology) for providing experiment equipment to accomplish the project.

References

[1] Korkut Ihsan. A dynamometer design and its construction for milling operation. Mater Des 2003;24(8):631–7.
[2] de Lacalle Luis Norberto López, Lamikiz A, Sánchez JA, de Bustos Igor Fernándezs. Simultaneous measurement of forces and machine tool position for diagnostic of machining tests. IEEE Trans Instrum Meas 2005;54(6):2329–35.
[3] Seguy Sébastien, Campa Francisco Javier, De Lacalle Luis Norberto López, Arnaud Lionel, Dessein Gilles, Aramendi Gorka. Toolpath dependent stability lobes for the milling of thin-walled parts. Int J Mach Machinability Mater 2008;4(4):377–92.
[4] Baohai Wu, Xue Yan, Ming Luo, Ge Gao. Cutting force prediction for circular end milling process. Chin J Aeronaut 2013;26(4):1057–63.
[5] Han Xiong, Tang Limin. Precise prediction of forces in milling circular corners. Int J Mach Tools Manuf 2015;88:184–93.
[6] Yaldız Süleyman, Ünsaçar Faruk. Design, development and testing of a turning dynamometer for cutting force measurement. Mater Des 2006;27(10):839–46.
[7] Teti R, Jemielniak K, O'Donnell G, Dornfeid D. Advanced monitoring of machining operations. CIRP Ann-Manuf Technol 2010;59(2):717–39.
[8] Franco-Gasca Luis Alfonso, Herrera-Ruiz Gilberto, Vera Rocío Peniche, Troncoso René de Jesús Romero, Leal-Tafolla Wbaldo. Sensorless tool failure monitoring system for drilling machines. Int J Mach Tools Manuf 2006;46(3):381–6.
[9] Bin Li, Chen Zhang, Hongqi Liu. Indirect measurement of the milling forces based on spindle motor current. J Huazhong University Sci Technol (Nat Sci Ed) 2008;36(3):5–7.
[10] Li Xiaoli, Ouyang Gaoxiang, Liang Zhenhu. Complexity measure of motor current signals for tool flute breakage detection in end milling. Int J Mach Tools Manuf 2008;48(3):371–9.
[11] Sevilla-Camacho PY, Herrera-Ruiz G, Robles-Ocampa JB, Jáuregui-Correa JC. Tool breakage detection in CNC high-speed milling based in feed-motor current signals. Int J Adv Manuf Technol 2011;53(9-12):1141–8.
[12] Karabay Sedat. Analysis of drill dynamometer with octagonal ring type transducers for monitoring of cutting forces in drilling and allied process. Mater Des 2007;28(2):673–85.
[13] Yaldiz Süleyman, Ünsaçar Faruk, Saglam Haci, Isik Hakan. Design, development and testing of a four-component milling dynamometer for the measurement of cutting force and torque. Mech Syst Signal Process 2007;21(3):1499–511.
[14] Totis G, Sortino M. Development of a modular dynamometer for triaxial cutting force measurement in turning. Int J Mach Tools Manuf 2011;51(1):34–42.
[15] Ma Lei, Melkote Shreyes N, Morehouse John B, Castle James B, Fonda James W, Johnson Melissa A. Thin-film PVDF sensor-based monitoring of cutting forces in peripheral end milling. J Dyn Syst Meas Contr 2012;134(5):05–14.
[16] Klocke F, Gierlings S, Adams O, Auerbach T, Kamps S, Veselovac D, et al. New concepts of force measurement systems for specific machining processes in aeronautic industry. In: Fifth CIRP conference on high performance cutting, vol. 1. 2012. p. 552–57.
[17] Zhaoyan Liu, Zhenshan Lei. Measurement technique of cutting force by using fiber Bragg grating and virtual instrument. Tool Eng 2005;39(10):53–6.
[18] Liu Mingyao, Zhou Zude, Tao Xiaoliang, Tan Yuegang. A dynamometer design and analysis for measurement the cutting forces on turning based on optical fiber Bragg Grating sensor. IN: Tenth world congress on intelligent control and automation; 2012. p. 4287–90.
[19] Dongsheng Li, Hongnan Li. Strain transfer analysis of embedded fiber Bragg grating sensors. Chin J Theor Appl Mech 2005;37(4):435–40.
[20] Arizmendi M, Campa FJ, Fernández J, López de Lacalle LN, Gil A, Bilbao E, et al. Model for surface topography prediction in peripheral milling considering tool vibration. CIRP Ann-Manuf Technol 2009;58(1):93–6.